Raman spectroscopy of filamentous bacteriophage Ff (fd, M13, f1) incorporating specifically-deuterated alanine and tryptophan side chains

Assignments and structural interpretation

Kelly L. Aubrey and George J. Thomas, Jr.
Division of Cell Biology and Biophysics, School of Basic Life Sciences, University of Missouri at Kansas City, Kansas City, Missouri 64110

ABSTRACT Structural interpretation of the Raman spectra of filamentous bacteriophages is dependent upon reliable assignments for the numerous Raman vibrational bands contributed from coat protein and packaged DNA of the virion. To establish unambiguous assignments and facilitate structural conclusions derived from them, we have initiated a systematic study of filamentous bacteriophage Ff (fd, f1, M13) incorporating protein subunits with specifically deuterated amino-acid side chains. Here, we report and interpret the Raman spectra of fd virions which incorporate: (*a*) a single deuterio-tryptophan residue per coat protomer [fd(W_{d5})], (*b*) ten deuterio-alanines per protomer [fd($10A_{d3}$)], and (*c*) both deuterio-tryptophan and deuterio-alanine [fd(W_{d5} + $10A_{d3}$)]. The unambiguous assignment of coat protein Raman bands in normal and deuterated isotopomers of fd establishes the validity of earlier empirical assignments of many key Raman markers, including those of packaged ssDNA (Thomas et al., 1988). Present results confirm that deoxyguanosine residues of the packaged ssDNA molecule depart from the usual C2′-endo/anti conformation characteristic of protein-free DNA in aqueous solution, although C2′-endo/anti conformers of thymidine are not excluded by the data. The combined results obtained here on normal fd, and on fd incorporating deuterio-tryptophan [fd(W_{d5}) and fd(W_{d5} + $10A_{d3}$)], show also that the microenvironment of the single tryptophan residue per coat protomer (W26) can be clearly deduced as follows: (*a*) The indole 1-NH donor group of each protomer in fd forms a moderately strong hydrogen bond, most likely to a hydroxyl oxygen acceptor. (*b*) The planar indole ring exists in a hydrophilic environment. (*c*) The torsion angle describing the orientation of the indole ring (C3-C2 linkage) with respect to the side-chain (Cα-Cβ bond) is unusually large, i.e., $|X^{2,1}| \sim 120°$. With respect to alanine isotopomers, the present results show that alanine residues, and possibly other methyl-containing side chains, are significant contributors to the fd Raman spectrum. The present study provides new information on protomer side chains of fd and demonstrates a Raman methodology which should be generally useful for investigating single-site interactions and macromolecular conformations in other nucleoprotein assemblies.

INTRODUCTION

Ff is the class prototype of long (~880 nm) and thin (~7 nm diameter) bacteriophage filaments which are assembled as a protein cylinder packaging a single-stranded DNA loop. The filamentous phages fd, f1, and M13 are closely similar members of the Ff class, also referred to as class I. The ssDNA genome of fd contains 6,408 nucleotides and constitutes ~12% of the total virion mass of 16.4×10^6 D. The protein sheath of fd comprises ~2,750 copies of a subunit of 50 amino acids, the product of viral gene 8 (gpVIII) which serves as the major coat protein, and a few copies of four minor proteins located at the filament ends. Fiber x-ray diffraction shows that the sheath of gpVIII protomers is arranged with five-fold rotational symmetry and an approximate two-fold screw axis (Marvin et al., 1974*a*; Marvin et al., 1974*b*; Makowski and Caspar, 1981). Comprehensive reviews of the molecular biology and morphogenesis of filamentous phages have been given (Denhardt et al., 1978; Webster and Lopez, 1985; Model and Russel, 1988).

A large body of structural work exists for phage fd, including studies based upon fiber x-ray diffraction, solid-state nuclear magnetic resonance (NMR) and solution-state Raman, infrared, fluorescence and CD spectroscopies. This work has been reviewed (Makowski, 1984; Opella et al., 1987; Thomas, 1987; Day et al., 1988*a*), and a model consistent with the body of diffraction and spectroscopic results has recently been proposed (Marvin, 1989, 1990). An important structural characteristic of fd, confirmed by all experimental data, is the prevalence of α-helical secondary structure in coat protein subunits. Less studied is the secondary structure of packaged fd DNA. In a comparison of both class I (fd, If1, IKe) and class II (Pf1, Xf, Pf3) virions, a number of low-intensity Raman bands could be assigned to the packaged viral DNA's (Thomas et al., 1983). Many differences were apparent between different filamentous viruses, indicating that the packaged ssDNA structures were not the same. Additionally, all differed from protein-free ssDNA in solution, with regard to nucleo-

This article represents part XXXIV in the series, Studies of Virus Structure by Laser Raman Spectroscopy.
Address correspondence to Dr. Thomas.

side sugar pucker and backbone phosphodiester geometry (Thomas et al., 1988), implying specific protein-DNA interactions. Complementary Raman studies of Hg(II) binding to the packaged ssDNA of these phages confirm the diversity of their ssDNA conformations and subunit interactions (Day et al., 1988*b*) but provide few details of the interaction sites. At present, relatively little is known about the nature of protein-DNA interactions or protomer side-chain packing in assembled virions.

Raman spectroscopy has been one of the more extensively applied methods for investigating solution structures of filamentous bacteriophages (Thomas and Murphy, 1975; Thomas et al., 1983; Thomas et al., 1988; Day et al., 1988*b*; and references therein). The spectra are rich in the number of well-resolved bands contributed by protein and DNA subgroups of the phage, and in the diversity of spectra manifested for different experimental conditions. These characteristics favor the use of Raman spectroscopy for elucidating interactions at many different molecular sites of the protomers (Marvin, 1990) and genome (Thomas et al., 1988) and investigating conformational transitions accompanying changes in phage environment (Thomas et al., 1983). Yet, only a fraction of the potentially informative Raman bands of filamentous bacteriophages has so far been exploited for structural conclusions. A major reason is the prerequisite for unambiguous band assignments. The number of definitive assignments can be advanced by comparisons with model compounds of known Raman signature, and especially by the introduction of site-specific modifications which perturb vibrational dynamics in a predictable manner without significantly altering conformations or assembly characteristics of virion components. Accordingly, site-specific isotope substitution is the method of choice for advancing Raman spectral assignments and promoting structural conclusions therefrom. Previously, we utilized this approach by incorporating deuterio-tyrosine and deuterio-phenylalanine residues into coat proteins of phage fd (Thomas et al., 1988). The initial results corroborated key Raman assignments for aromatic residues and permitted conformational inferences about the packaged ssDNA.

In the present work, we begin a more systematic and comprehensive approach to achieving definitive Raman band assignments for the fd virion by introducing deuterated tryptophan and deuterated alanine residues, separately and in combination, into gpVIII of the mature phage assembled in vivo. Attention is focused on these residues for the following reasons. The gpVIII protomer contains a single tryptophan (W26) which is believed to fulfill a critical role in stabilizing the virion. Efforts to substitute other amino acids for W26 by site-directed mutagenesis do not yield viable phage (A. Kuhn, personal communication); although the mutations allow membrane insertion, they inhibit phage assembly. Recently, Raman bands of the amino acid L-tryptophan have been analyzed in detail with respect to their conformational dependencies (Takeuchi and Harada, 1986; Harada et al., 1986; Miura et al., 1988, 1989). Therefore, reliable Raman assignments for the W26 residue in fd coat protein can be expected to provide new insights into several structural aspects of the virion, including: (*a*) the hydrogen bonding role of the indole 1N-H donor group, (*b*) the hydropathic environment of the indole ring, and (*c*) the torsion angle $X^{2,1}$, which describes indole ring orientation with respect to the protomer main chain. This information, in turn, can aid in distinguishing domains of the protomer which may be important for membrane insertion, or for DNA coating and uncoating reactions (Kuhn et al., 1990). Finally, we note that many intense Raman bands of the normal tryptophan residue of fd coincide with the region of the Raman spectrum (600–900 cm^{-1}) containing conformation-sensitive bands of packaged ssDNA. We expect the Raman bands of the deuterio-tryptophan residue to be isotope-shifted outside of this key spectral interval (Bunow and Levin, 1977; O'Leary and Levin, 1986), thus permitting direct verification of previously proposed conformational features of the packaged fd genome (Thomas et al., 1988).

Alanine, on the other hand, is the most abundant amino acid of gpVIII, constituting 20% of the 50 residues. As shown in Fig. 1, it is distributed widely through the protomer sequence (A1, A7, A9, A10, A16, A18, A25, A27, A35, A49). Specific Raman contribu-

a ^{1}AEGDDPAKAAFDSLQASATEYIGYAWAMVVVIVGATIGIKLFKKFTSKAS^{50}

b

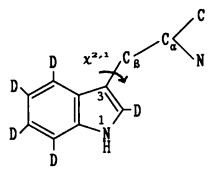

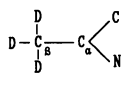

FIGURE 1 (*a*) Amino acid sequence of the fd coat protein, gpVIII. Tryptophan (W26) and alanine (A1, A7, A9, A10, A16, A18, A25, A27, A35, A49) residues employed as deuterium labels are underlined. (*b*) Covalent structures of tryptophan-d_5 and alanine-d_3 indicating sites of deuterium substitutions. The side-chain torsion angle $X^{2,1}$ of tryptophan is also indicated.

tions of alanine are of considerable general interest because scant information is available on methyl group modes in native proteins. Recent normal mode analysis of the alanine tripeptide underscores the limited experimental data available on alanine residues of native proteins (Qian et al., 1991). Knowledge of vibrational modes of the alanine side chains of fd should also be useful in identifying bands of other methyl-containing aliphatic side chains (viz. V, I, L, T, and M) of gpVIII.

The present procedures incorporate the deuterium isotopomers L-tryptophan-2′,4′,5′,6′,7′-d_5 and L-alanine-3,3,3-d_3 (Fig. 1), singly and in combination, into the fd coat protein during in vivo assembly. The labeled bacteriophage, designated fd(W_{d5}), fd($10A_{d3}$) and fd(W_{d5} + $10A_{d3}$), were purified and harvested in quantities sufficient for Raman spectroscopy (Aubrey, 1990). Similar methods have been employed to label fd protomers for solid-state NMR analysis (Cross et al., 1983; Opella et al., 1987).

EXPERIMENTAL PROCEDURES

Sample preparations and purification

The specifically deuterated amino acids, L-tryptophan-2′,4′,5′,6′,7′-d_5 (W_{d5}) and L-alanine-3,3,3-d_3 (A_{d3}), were obtained from Merck, Sharp and Dohme Isotopes (Rahway, NJ). Normal L-amino acids and standard reagents were obtained from Sigma Chemical Co. (St. Louis, MO). Growth media were obtained from Difco Laboratories (Grand Island, NY). Bacteriophage fd was grown on *Escherichia coli* strain Hfr3300, obtained from Dr. Loren A. Day, Public Health Research Institute (New York, NY). Mature viral particles, extruded through the bacterial cell wall and into the growth medium, were collected by precipitation with polyethylene glycol (20 g/l) and NaCl (0.5 M). The precipitate was purified by resuspension in 10 mM tris buffer at pH 7.7 and subjected to two or more cycles of differential sedimentation, consisting of clarifying spins at 20,000 rpm for 20 min and pelleting spins at 40,000 rpm for 2 h. Yields of virus ranged from 25 to 40 mg/l culture medium and plating efficiencies ranged from 0.2 to 0.6 pfu per virion particle.

Ordinarily, the purified virus pellet was used directly for Raman spectroscopy by transferring 10 μl portions to glass capillary tubes (Kimax #34507) employed as Raman sample cells. This procedure yielded Raman samples with virus concentrations in the range 50 to 80 mg/ml, as determined by UV absorbance measurements (model DU-50 spectrometer; Beckman Instruments Inc., Fullerton, CA) on aliquots diluted 1:1000 in 10 mM tris buffer. We asumed for fd an extinction coefficient of 3.84 mg^{-1} cm^2 at 269 nm. Additionally, samples were prepared for Raman spectroscopy with precise control of buffer concentration as follows. Equilibrium dialysis of representative samples was carried out against pH 7.7 tris buffer using 6,000–8,000 MW tubing (No. 08-670A; Fisher Scientific Co., Pittsburgh, PA) before concentrating the sample by high-speed centrifugation. Raman spectra reported below for fd and its isotopomers are for solutions with pH in the range 7.7–7.9, quoted nominally as 7.8. Raman spectra of A_{d3} and A were obtained from aqueous solutions at 100 mg/ml and pH 7.8. Because W_{d5} and W have very low solubility near pH 7, Raman spectra were collected from pH 10 solutions (60 mg/ml), as well as from solid samples.

To incorporate deuterated amino acids into the coat protein of fd, the host was infected in M9 minimal medium supplemented with the appropriate deuterio-labeled amino acid(s) at 0.1 mM (per residue in gpVIII). The medium also contained 10 μg/ml thiamine-HCl, 1% glycerol and all other L-amino acids combined at 2 mM. Virus infection and subsequent isolation and purification were carried out in the same manner as with growth of normal phage. Typical phage yields were 5–10 mg/l culture medium and plating efficiencies were 0.4–0.8 pfu/virion. As before, Raman sample concentrations were determined to be in the range 50–80 mg/ml. Separate protocols were carried out to incorporate either W_{d5} [fd(W_{d5})], or A_{d3} [fd($10A_{d3}$)], or both W_{d5} and A_{d3} [fd(W_{d5} + $10A_{d3}$)].

The extent of incorporation of specifically-deuterated amino acids was assayed (Raman) spectrophotometrically by observing specific C-D stretching bands of the labeled viruses. In the case of fd(W_{d5}), the deuterated indole ring exhibits characteristic aromatic C-D stretching bands of relatively low intensity at 2,264 and 2,294 cm^{-1}. These bands are broad and presumably represent composites of two or three distinct C-D bond-stretching modes. The same broad bands are observed in the deuterated amino acid. Normal tryptophan and normal fd exhibit corresponding C-H stretching bands near 3,058 and 3,065 cm^{-1} (3058 ÷ 2264 = 1.35; 3065 ÷ 2294 = 1.34). For fd($10A_{d3}$), deuteriomethyl symmetric stretching (2,082 and 2,124 cm^{-1} Fermi doublet) and asymmetric stretching (2,246 cm^{-1}) are more intense and easily detected (Bellamy, 1980; Bunow and Levin, 1977), as are their C-H counterparts in normal alanine and normal fd (2,874, 2,920, 2,943 cm^{-1}). The alanine deuteration shifts are, respectively, 1.38, 1.37, and 1.31. The assignment of the weak shoulder near 2,144 cm^{-1} in fd($10A_{d3}$) is not straightforward, because several fundamental combinations could generate this low intensity feature. For fd(W_{d5} + $10A_{d3}$), both sets of C-D stretching bands are observed, as shown in Fig. 2. (See also Fig. 6). In all cases, the extent of labeling appears to be essentially stoichiometric, i.e., ≥95%. Normal tryptophan and alanine could not be detected in the fd isotopomers, as judged by the following criteria: (*a*) Raman bands of normal A and W could not be observed above the contributions from nonlabeled side chains; and (*b*) a 10-fold increase of the amount of deuterio-labeled amino acid in the growth medium resulted in no significant increase in the intensity of any C-D marker band.

Raman spectroscopy

Virus and amino acid samples were sealed in glass capillary tubes for Raman analysis. Spectra were excited with the 514.5 nm argon laser line (Innova 70, Coherent Inc., Palo Alto, CA) and collected on a scanning double spectrometer (Ramalog V/VI, Spex, Inds., Inc., Edison, NJ) under the control of an IBM microcomputer (Li et al., 1981). Spectral resolution of 8 cm^{-1} and photon-counting integration of 1.5 s at 1.0 cm^{-1} intervals were employed. To improve signal-to-noise ratios, samples were scanned repetitively and individual scans were displayed and examined before averaging. All Raman spectra were collected at the ambient temperature of the laser-illuminated sample cell, i.e., 32° C, or on a jacketed cell thermostated at 10° C. The spectrometer wavenumber drive was calibrated to within ± 0.5 cm^{-1}, with indene as the primary standard and CCl_4 as a secondary standard. Spectra of normal and deuterated viruses and amino acids were recorded separately with 0.05 M Na_2SO_4 added for use of its prominent 980 cm^{-1} Raman band as an internal frequency standard. The reported Raman frequencies from signal-averaged spectra (up to 30 repetitive scans) are believed accurate to ±1.0 cm^{-1}, unless indicated otherwise. Crystalline samples were illuminated with laser power of 80–100 mW and solution samples with 100–200 mW.

Spectral subtractions to visualize band deuteration shifts were carried out with SpectraCalc software. Ordinarily these were performed on the raw data before solvent or background correction. This allowed differentiation of subtle changes that might otherwise have been difficult to detect, and avoided introduction of artifacts from

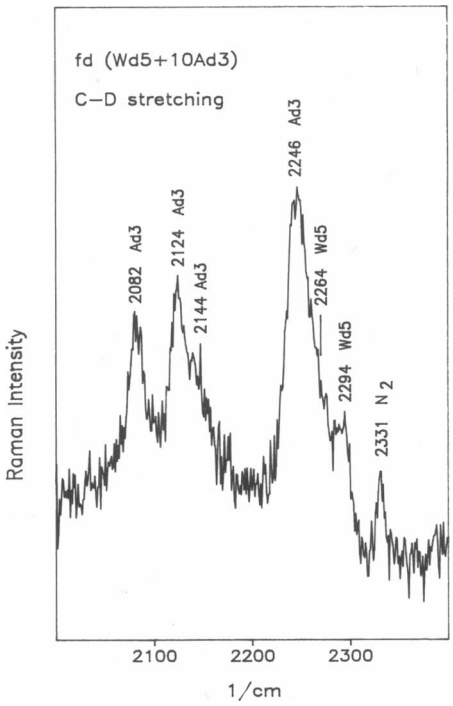

FIGURE 2 Raman spectrum in the region 2,000–2,400 cm^{-1} of fd(W_{d5} + 10A_{d3}) showing C-D stretching bands of the labeled side chains. The bands of A_{d3} (2,082, 2,124, 2,144, and 2,246 cm^{-1}) dominate this spectral interval, whereas the composite bands of W_{d5} (2,264, and 2,294 cm^{-1}) are relatively weak. The Raman-active stretching mode of ambient N_2 (2,331 cm^{-1}) serves as a convenient frequency standard. The spectrum shown is an average of five scans, uncorrected for solvent or background. Other details of the data collection protocol are discussed in the text.

incomplete solvent or background compensation in either minuend or subtrahend. Generally, the deuterated sample was employed as minuend, and the normal sample as subtrahend. In some cases, computer-averaged spectra were corrected for the buffer background by subtracting the Raman spectrum of 10 mM tris solution. This procedure compensates optimally for the intense Raman scattering from OH stretching modes in the 3,200–3,600 cm^{-1} region and for the much weaker but still significant bands of water in the 300–1,800 cm^{-1}. The data in the region 600–900 cm^{-1} are not particularly sensitive to the scaling factor employed in buffer subtraction (Thomas et al., 1983). Linear baseline corrections were also performed on some of the spectra in order to facilitate intensity comparisons. Typically, the lowest number of tangent points consistent with a horizontal baseline was employed. All other data refinements were performed with software developed in our laboratory.

RESULTS AND DISCUSSION

Spectral assignments of deuterated tryptophan and alanine side chains

Fig. 3 compares Raman spectra in the region 300–1,800 cm^{-1} for bacteriophage fd and the specifically-deuterated isotopomers, fd(W_{d5}), fd(10A_{d3}) and fd(W_{d5} + 10A_{d3}). These and all subsequent data were collected from virus solutions in 10 mM tris buffer, without added NaCl or other salts, which corresponds to the low-to-medium salt conditions described previously for fd (Thomas et al., 1983). Raman band intensities show relatively little ionic-strength dependence at these salt conditions, although significantly different Raman profiles are observed at higher NaCl concentrations (>0.2 M NaCl) (Thomas et al., 1983). Fig. 3 is labeled (↓) to identify the Raman bands of normal fd which decrease either significantly or altogether with incorporation of deuterated tryptophan or alanine. The corresponding Raman intensity increases generated in spectra of fd(W_{d5}), fd(10A_{d3}) and fd(W_{d5} + 10A_{d3}), representing bands of the deuterium-labeled side chains, are also designated (↑) in Fig. 3. These characteristics can be more clearly visualized in the difference spectra of Figs. 4 and 5.

We note that the 300–1,800 cm^{-1} fingerprint region of fd exhibits eight distinct bands which are eliminated (or diminished) by deuteration of the W26 side chain. These are replaced by 11 well-resolved bands in fd(W_{d5}). On the other hand, only three bands of fd are significantly affected by deuteration of the 10 alanine side chains, giving rise to four new bands in fd(10A_{d3}). The dominating effect of tryptophan deuteration is consistent with the larger number of normal modes of high Raman cross section anticipated for the aromatic indole ring in comparison to the lower Raman intensities expected for deformation modes of the aliphatic (CH_3 or CD_3) side chain. Also as expected, all of the deuteration-sensitive W and A bands are eliminated (or diminished) in the double derivative, fd(W_{d5} + 10A_{d3}), the spectrum of which shows the anticipated 15 new bands. In addition, we find six bands in the region 2,000–2,400 cm^{-1} assignable in straightforward manner to either W_{d5} or A_{d3} residues of fd(W_{d5} + 10A_{d3}) (Fig. 2). All assignments are summarized in Table 1. The consistency of the results on fd(W_{d5}), fd(10A_{d3}) and fd(W_{d5} + 10A_{d3}) confirms the qualitative accuracy of the assignments (Table 1) and the quantitative incorporation of deuterium labels.

The band shifts induced in the Raman spectrum of fd by incorporation of W_{d5} and A_{d3} are confirmed independently by Raman spectra of the labeled amino acids (data not shown). Our results on W_{d5} are also consistent with published data on deuterated indoles (Takeuchi and Harada, 1986).

Region 600–900 cm^{-1}: resolution of Raman bands of tryptophan and packaged fd DNA

Fig. 4 shows Raman spectra of phage fd, fd(W_{d5}), fd(10A_{d3}) and fd(W_{d5} + 10A_{d3}) in the spectral region

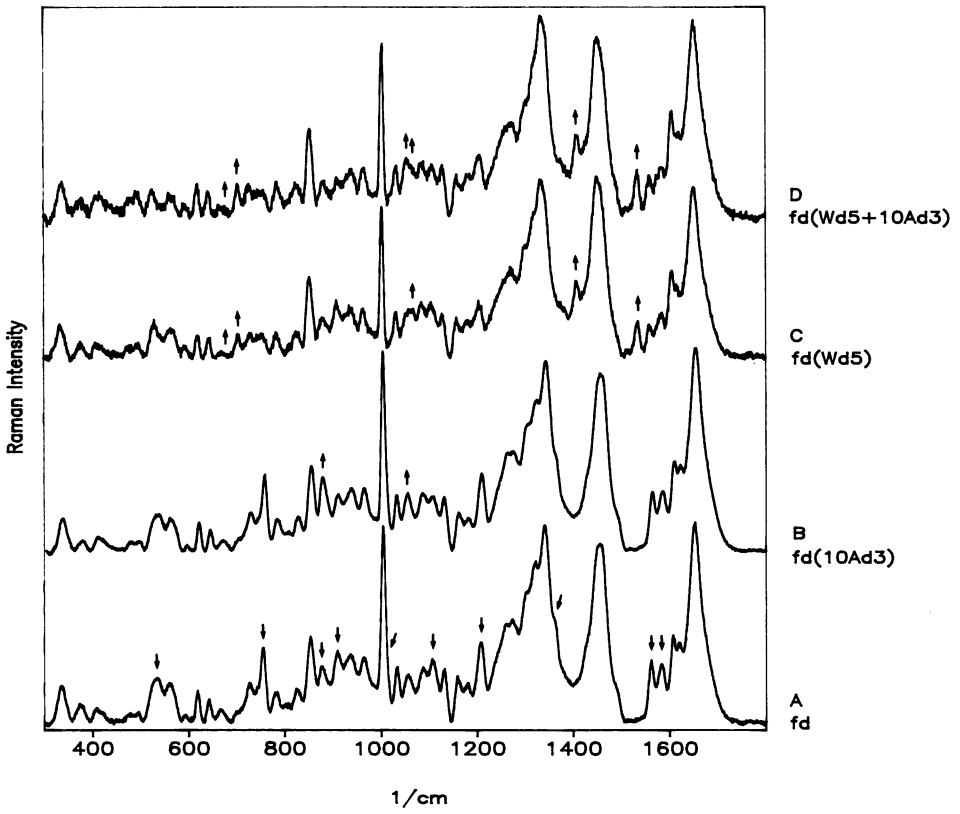

FIGURE 3 Raman spectra in the region 300–1,800 cm^{-1} of normal fd and its isotopomers, fd(W_{d5}), fd($10A_{d3}$) and fd(W_{d5} + $10A_{d3}$), as indicated. Phage are dissolved at 80 mg/ml in 10 mM tris, pH 7.8 and 32° C. Each spectrum is the average of eight scans and is corrected for the solvent background. Downward-pointing arrows in the fd spectrum mark bands contributed by W and/or A which are eliminated, shifted in frequency, or diminished in intensity by incorporation of labeled side chain(s). Upward-pointing arrows indicate bands in the isotopomer spectra assigned to W_{d5} and A_{d3} which are generated by the labeled side chains, in accordance with the assignments of Table 1.

600–900 cm^{-1}. This spectral region is expected to contain conformation-sensitive marker bands of the packaged fd genome, as well as intense bands from tyrosine (Y21 and Y24) and tryptophan (W26) residues of the gpVIII protomer. Although the DNA bands in this region are intrinsically intense, the overwhelming coat protein content of the phage (~88%) renders them relatively weak by comparison. Of particular interest is the weak band at 806 cm^{-1}, assigned previously to the DNA backbone on the basis of its invariance to deuterations in tyrosine and phenylalanine (Thomas et al., 1988). Expanded scale spectra of fd(W_{d5}), fd($10A_{d3}$) and fd(W_{d5} + $10A_{d3}$) (not shown) confirm also that no intensity change occurs at 806 cm^{-1} with tryptophan and alanine deuterations, even though the band is largely overlapped in spectra of the deuterio-tryptophan isotopomers by the W_{d5} band ca. 817 cm^{-1} (Table 1). (Note that the 817 cm^{-1} band of W_{d5} tends to fill in the minimum on the high frequency side of the 806 cm^{-1} band, as shown in Fig. 4, traces *C* and *D*.) Complete assignments are included in Table 1. Additional deuteration characteristics of the tyrosine and phenylalanine bands in this region have also been discussed (Thomas et al., 1988).

Fig. 4 shows that the intense tryptophan band at 756 cm^{-1} in the spectrum of normal fd is largely eliminated in the spectrum of fd(W_{d5}), thereby exposing an underlying weaker band near 750 cm^{-1}, which we assign in whole or in part to packaged DNA. Note that the extent of incorporation of W_{d5} permits ruling out significant residual intensity near 750 cm^{-1} from normal tryptophan. (See Experimental Methods.)

Fig. 4 also shows that the intensity of the prominent tryptophan band at 876 cm^{-1} in the spectrum of fd is reduced about two-fold in the spectrum of fd(W_{d5}). Although the packaged ssDNA is expected to exhibit a weak band near 880–890 cm^{-1} (Benevides et al., 1991a), the residual 880 cm^{-1} intensity observed here is too great to be attributed entirely to DNA. In this case, we assign most of the intensity which remains at 880 cm^{-1} in the spectrum of fd(W_{d5}) to the deuterated tryptophan ring itself. These findings are in accord with reported spec-

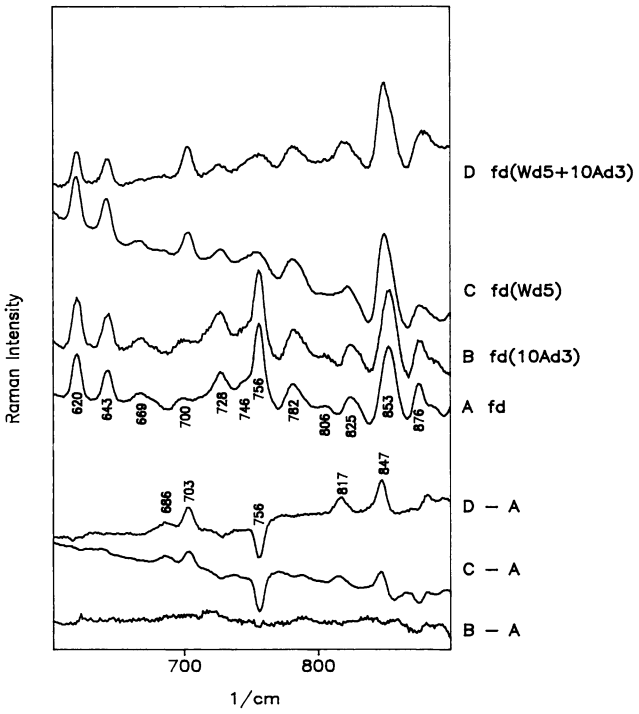

FIGURE 4 Raman spectra in the region 600–900 cm^{-1} of: (*A*) normal fd, (*B*) fd(A_{d3}), (*C*) fd(W_{d5}), and (*D*) fd(W_{d5} + $10A_{d3}$); obtained at the same conditions indicated in Fig. 3. To preserve natural band shapes, the spectra have not been corrected for solvent background or otherwise refined. Traces A, B, C and D are averaged from (up to 70) multiple scans. The lower three traces show on an expanded ordinate scale difference spectra computed with a deuterium isotopomer as minuend and normal fd as subtrahend. For computation of difference spectra, intensities were scaled to compensate the bands at 620 (phenylalanine) and 643 cm^{-1} (tyrosine), which are invariant to the isotope substitutions. Features in the difference spectra which do not exhibit signal-to-noise ratios > 2, or which occur on the steeply sloping contours of sharp bands, are not considered significant. Principal Raman bands discussed in the text are labeled in cm^{-1} units.

tral data and normal coordinate analyses of deuterated indoles (Takeuchi and Harada, 1986), which show that the ring mode at 756 cm^{-1} is highly sensitive to ring perdeuteration, while modes between 850 and 900 cm^{-1} are less so. Tryptophan contributes no other significant Raman intensity in the region 600–900 cm^{-1}. The tryptophan deuteration effects revealed in Fig. 4, and particularly the absence of frequency shifts in bands assigned previously to DNA base and phosphate groups provide full confirmation of previous DNA assignments (Thomas et al., 1988).

On the basis of the present results and those described previously (Thomas et al., 1988), we identify six bands in the 600–900 cm^{-1} region as being due mainly or entirely to the packaged ssDNA molecule. The assigned DNA Raman frequencies and their conformational implications are summarized in Table 2.

Other deuteration-sensitive Raman bands of tryptophan and alanine

The incorporation of W_{d5} diminishes intensities of the well-resolved bands of fd at 1,560 and 1,582 cm^{-1}. Additionally, significant changes occur in the complex band shapes near 1,002, 1,206, and 1,360 cm^{-1}, by virtue of deuteration shifts in the underlying bands of W at 1,012, 1,206 and 1,360 cm^{-1} (Fig. 5). The corresponding Raman frequencies for the W_{d5} residue are listed in Table 1. These results are in full agreement with reported spectra and normal mode calculations for indole and its deuterium isotopomers (Takeuchi and Harada, 1986). The results of fd(W_{d5}) demonstrate that the tryptophan ring can be expected to generate a Raman band at 1,206 cm^{-1} in other proteins. The 1,206 cm^{-1} band of fd, assigned previously to tyrosine residues (Thomas et al., 1983), shows a significant intensity decrease upon W_{d5} incorporation. This confirms the 1,206 cm^{-1} contribution of W26, not recognized in earlier fd studies, but clearly supported by results obtained on model compounds (Takeuchi and Harada, 1986).

Alanine contributes two well-resolved bands to the Raman spectrum of normal fd at 908 and 1,105 cm^{-1}. The spectrum of fd($10A_{d3}$) shows that both bands are largely eliminated upon incorporation of A_{d3} into coat protein subunits. Because the 908 cm^{-1} mode is expected to involve primarily N-Cα-Cβ bond stretching (Qian et al., 1991), only a small deuteration shift is anticipated. Accordingly, the corresponding mode for the deuterium isotopomer is reasonably assigned to the band at 891 cm^{-1}. For the 1,105 cm^{-1} mode, Cα-Cβ-H valence angle bending is expected to be a major constituent (Qian et al., 1991); therefore a larger deuteration shift is anticipated. Either the 946 or the 1,021 cm^{-1} mode, or both, are likely candidates for the corresponding vibration(s) in fd($10A_{d3}$). We also find that the alanine methyl group contributes a band ~1,457 cm^{-1}, which appears as a poorly resolved shoulder to the much more intense Raman band near 1,450 cm^{-1}. The shoulder is significantly reduced in intensity in fd($10A_{d3}$), but not entirely eliminated. This is as expected because a substantial number of protomer methyl side chains (4V + 4I + 3T + 2L + M) remains in the alanine-labeled phage. In accordance with model compound studies, the 1,457 cm^{-1} shoulder in the spectrum of fd can be attributed unambiguously to a hydrogenic mode, i.e., CH_3 asymmetric bending (Bellamy, 1980; Qian et al., 1991). The corresponding CD_3 mode should occur near 1,057 cm^{-1} (1460 ÷ 1.38). We

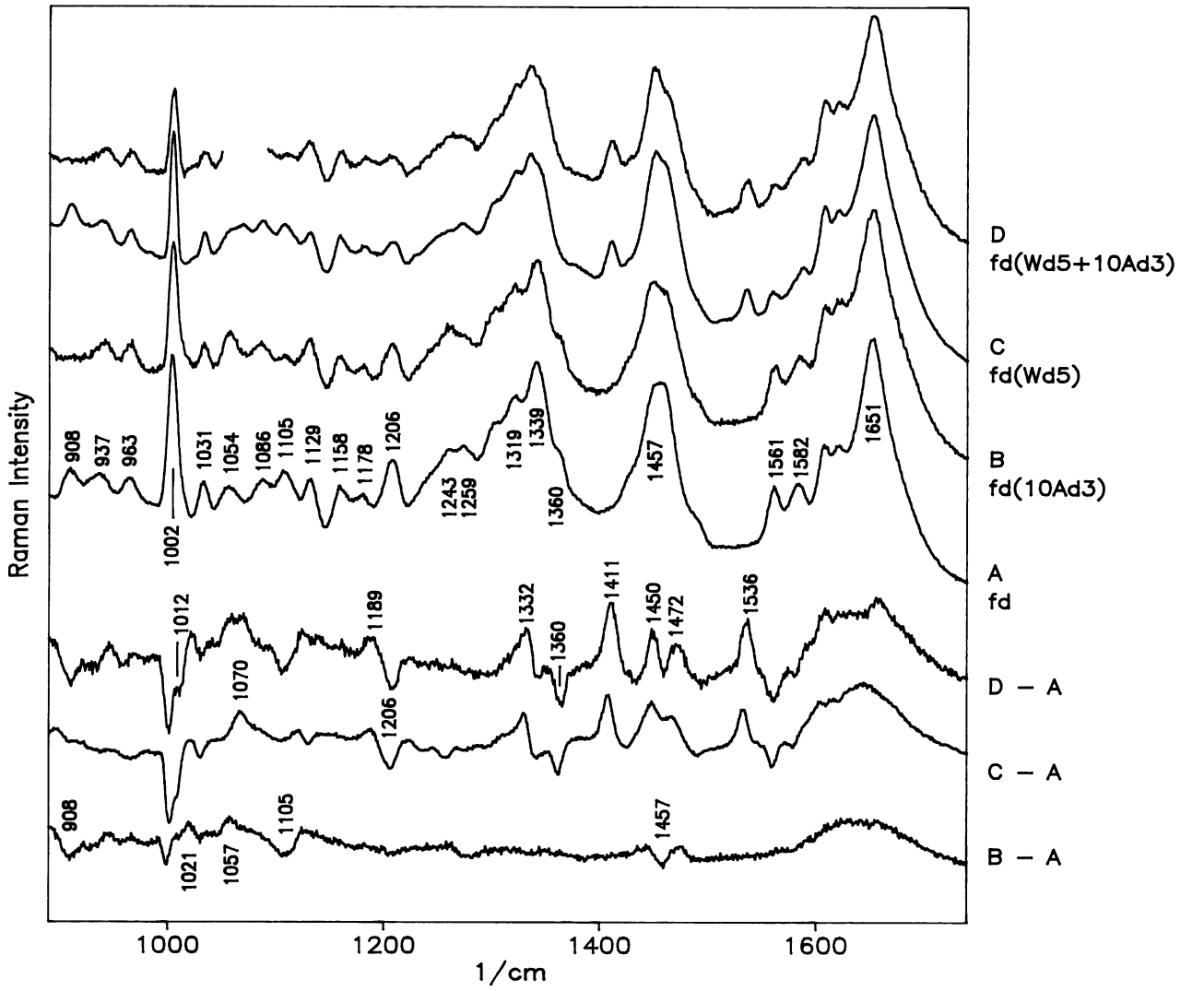

FIGURE 5 Raman spectra in the region 900–1,750 cm^{-1} of: (*A*) normal fd, (*B*) fd(A_{d3}), (*C*) fd(W_{d5}), and (*D*) fd(W_{d5} + $10A_{d3}$); obtained and presented as indicated in Fig. 4. For computation of difference spectra, intensities were scaled to compensate the amide I band at 1,651 cm^{-1}, which is invariant to the isotope substitutions. The very broad difference bands in the region above 1,600 cm^{-1} are due mainly to uncompensated H_2O. Principal Raman bands discussed in the text are labeled in cm^{-1} units.

therefore assign the 1,057 cm^{-1} band of fd($10A_{d3}$) to CD_3 asymmetric bending.

In the hydrogen-stretching region of the fd Raman spectrum, difference spectroscopy reveals the bands of the deuterium substituted CH groups. Thus, the difference spectrum fd-minus-fd(W_{d5}) reveals two bands assignable to W (3,058 and 3,065 cm^{-1}), and the difference spectrum fd-minus-fd($10A_{d3}$) reveals three bands from A (2,874, 2,920 and 2,943 cm^{-1}) (data not shown). The bands are absent from spectra of the labeled phage where they are replaced by the corresponding CD stretching bands, as shown in Fig. 6. Assignments for fd(W_{d5}), fd($10A_{d3}$) and fd(W_{d5} + $10A_{d3}$) are included in Table 1.

CONCLUSIONS

Environment of tryptophan-26 in fd

The single tryptophan residue (W26) of the fd coat protein is unusual in several respects. Studies by site-directed mutagenesis show that although a variety of mutations at different sites in viral gene VIII can lead to productive and apparently normal phage assembly (Kuhn

TABLE 1 Raman frequencies and assignments for normal fd and isotopomers fd(W_{d5}), fd($10A_{d3}$), and fd(W_{d5} + $10A_{d3}$)

Normal fd			cm^{-1}	cm^{-1}	cm^{-1}
cm^{-1}[a]	Intensity[b]	Assignment[c]	fd(A_{d3})	fd(W_{d5})	fd(W_{d5} + $10A_{d3}$)
336	(2.0)	skl	*d*	*d*	*d*
377	(0.9)	skl	*d*	*d*	*d*
411	(0.7)	skl	*d*	*d*	*d*
424	(0.5s)	skl	*d*	*d*	*d*
476	(0.4)	skl	*d*	*d*	*d*
493	(0.5)	thy,gua	*d*	*d*	*d*
528	(2.5)	skl;AmVII	*d*	*d*	*d*
536[W]	(2.5)	skl;W	*d*	*e*	*e*
559	(2.1)	AmVII;skl	*d*	*d*	*d*
568	(s)	AmVII	*d*	*d*	*d*
594	(0.3)	skl	*d*	*d*	*d*
620	(1.7)	F	*d*	*d*	*d*
643	(1.3)	Y	*d*	*d*	*d*
669	(0.7b)	thy,gua	*d*	*d*	*d*
—		W_{d5}	—	686	686
700	(0.5s)	AmV	d	*d*	*d*
—		W_{d5}	—	703	703
728	(2.2)	ade	*d*	*d*	*d*
746	(1.9s)	thy	*d*	*d*	*d*
756[W]	(4.2)	W	*d*	—	—
782	(1.6)	cyt	*d*	*d*	*d*
806	(1.0)	bk	*d*	*d*	*d*
—		W_{d5}	—	817	817
825	(1.8)	Y	*d*	*d*	*d*
—		W_{d5}	—	847	847
853	(4.7)	Y{f}	*d*	*d*	*d*
876[W]	(3.1)	W	*d*	*d*	*d*
890	(ws)	G;bk	*d*	*d*	*d*
—		A_{d3}	891	—	891
908[A]	(4.0)	A . . .	*e*	*d*	*e*
937	(3.8)	CCC def	*d*	*d*	*d*
—		A_{d3}	946	—	947
963	(3.6)		*d*	*d*	*d*
980	(s)	I	*d*	*d*	*d*
1002	(11.0)	F	*d*	*d*	*d*
1012[W]	(s)	W	*d*	—	—
—		A_{d3}	1021	—	1022
1031	(3.1)	CC,CN,CO str	*d*	*d*	*d*
1054	(2.7)	CC,CN,CO str	*d*	*d*	*d*
—		A_{d3}	1057	—	1058
1086	(3.1)	CC str;bk	*d*	*d*	*d*
—		W_{d5}	—	1068	1070
1105[A]	(3.5)	A . . .	e	*d*	*e*
1129	(2.9)	CC str	*d*	*d*	*d*
1158	(2.6)	CC str	*d*	*d*	*d*
1178	(2.2)	Y	*d*	*d*	*d*
—		W_{d5}	—	1188	1189
1206[W]	(4.5)	Y,W	*d*	*e*	*e*
1243	(w,s)	AmIII;thy,cyt	*d*	*d*	*d*
1259	(5.5)	AmIII;thy,ade	*d*	*d*	*d*
1272	(5.8)	AmIII;Y	*d*	*d*	*d*
1300	(7.3)	CH,CH_2 def	*d*	*d*	*d*
1319	(9.0)	CH_2 def	*d*	*d*	*d*
—		W_{d5}	—	1331	1332
1339	(11.1)	CH_2,CH_3 def;W	*d*	*e*	*e*
1360[W]	(5.9s)	W	*d*	—	—
—		W_{d5}	—	1409	1411
1428	(s)	CH_2,CH_3 def	*d*	*d*	*d*
—		W_{d5}	—	1449	1450

TABLE 1 continued

Normal fd			cm^{-1}	cm^{-1}	cm^{-1}
cm^{-1a}	Intensity[b]	Assignment[c]	$fd(A_{d3})$	$fd(W_{d5})$	$fd(W_{d5} + 10A_{d3})$
1450	(10.0)	CH_2,CH_3 def	*d*	*d*	*d*
1457^A	(10.0)	CH_3,CH_2 def	*e*	*d*	*e*
—		W_{d5}	—	1468	1472
1485	(2.3s)	ade,gua	*d*	*d*	*d*
—		W_{d5}	—	1534	1536
1560^W	(3.5)	W	*d*	*e*	*e*
1582^W	(3.2)	W;gua,ade	*d*	*e*	*e*
1606	(4.9)	F,Y	*d*	*d*	*d*
1619	(4.4)	Y	*d*	*d*	*d*
1651	(11.2)	AmI	*d*	*d*	*d*
—	(w)	A_{d3}[CD_3 str]	2082	—	2082
—	(w)	A_{d3}[CD_3 str]	2124	—	2124
—	(w)	A_{d3}	2144	—	2144
—	(w)	A_{d3}[CD_3 str]	2246	—	2246
—	(w,s)	W_{d5}[CD str]	—	2264	2264
—	(w)	W_{d5}[CD str]	—	2294	2294
2874	(w)	A . . . [CH_3 str]	2874	—	2874
2920	(>10)	A . . . [CH_3 str]	2920	—	2920
2943	(w)	A . . . [CH_3 str]	2943	—	2943
3058	(w)	W . . . [CH str]	—	3058	3058
3065	(w)	W . . . [CH str]	—	3065	3065

(*a*)Raman frequencies are reproducible to within ±1 cm^{-1}, except for broad or weak bands and shoulders (±2 cm^{-1}). Superscripts A and W indicate Raman bands which are either absent or of significantly reduced intensity in deuterated isotopomers. When both residues contribute, the larger contributor is listed first. (*b*) Intensities are relative to the band at 1450 cm^{-1} in normal fd, which is assigned an arbitrary intensity of 10.0. Abbreviations: *w* = weak, *s* = shoulder, *b* = broad. (*c*) Proposed assignments are indicated for gpVIII amino-acid side chains (1-letter symbols), main chain skeleton (skl), or amide modes (AmI, AmIII, AmV, AmVII); for DNA nucleotide bases (three-letter symbols) or backbone (bk); and for stretching (str) or deformation (def) vibrations of specific chemical groupings (CH = methyne, CH_2 = methylene, CH_3 = methyl, CC = carbon-carbon, et cetera). Where multiple assignees are proposed, they are listed in order of decreasing contribution. The ellipsis (. . .) indicates bands which are contributed by all methyl-containing side chains (10A + 4V + 4I + 3T + 2L + 1M), or all aromatic side chains (3F + 2Y + W), as appropriate to the context. (*d*) Indicates that a band of essentially identical frequency and intensity is present in the Raman spectrum of the deuterated isotopomer. (*e*) Indicates that a band of significantly diminished intensity is present at the same frequency in the Raman spectrum of the deuterated isotopomer. Bands so designated are believed to correspond to vibrations of different character than the corresponding modes of column 1, though accidentally degenerate with them. (See, for example, Takeuchi and Harada, 1986.) (*f*) The major contributor to the composite 853 cm^{-1} band is *Y*. (Siamwiza et al., 1975).

et al., 1990), mutation of W26 does not yield viable phage. The W26 → X mutants, though translated and capable of membrane insertion, are severely inhibited for phage assembly (A. Kuhn, personal communication). This suggests an important role for W26 in the fd assembly pathway, which could involve protomer recognition either of the ssDNA genome or of a DNA-associated factor, possibly in conjunction with extrusion of the nascent filament through the host membrane. Physical properties of the W26 residue in wild-type phage are also atypical. Fluorescence spectra of fd reveal a very high quantum yield for W26 (Day et al., 1979); and CD spectra indicate an exceptionally sharp band contributed by W26 in the near UV (Day and Wiseman, 1978). The present study unambiguously identifies bands in the Raman spectrum of fd at 536, 756, 876, 1,012, 1,206, 1,360, 1,560, and 1,582 cm^{-1} as originating in whole or in part from W26, and these frequencies are also in certain respects atypical of tryptophan residues in proteins. Specific structural correlations have been established for several Raman bands of tryptophan and we next apply these correlations to the bands of fd at 876, 1,360, and 1,560 cm^{-1}.

The tryptophan frequency at 876 cm^{-1}, correlated with normal mode 17 (σ_{17}) of indole, originates in large part from bending of the C4-C5-C6 linkages in the plane of the ring (Takeuchi and Harada, 1986). The Raman band corresponding to σ_{17} in proteins was proposed by Kitagawa and co-workers (Kitagawa et al., 1979) as being sensitive to the local environment of the tryptophan residue. More recently, a precise linear dependence of σ_{17} upon the strength of hydrogen bonding by the indole 1N-H donor group has been demonstrated (Miura et al., 1988). In the absence of hydrogen bonding (e.g., indole dissolved in nonpolar solvents), the band center occurs at its high frequency limit of 884 cm^{-1}. In the case of

TABLE 2 **Selected Raman frequencies, assignments and residue conformations of packaged fd DNA**

Packaged fd DNA cm^{-1}	Assignment	Conformation	Reference
	[dT	C2′-endo	Dijkstra et al., 1991
669[a]	[dG	C3′-endo	Thomas et al., 1988
728	dA	C2′ or C3′endo	Thomas et al., 1988
746[b]	dT	C2′-endo	Dijkstra et al., 1991
782	dC	C2′ or C3′-endo	Thomas et al., 1988
806[c]	OPO	*gauche*$^-$/*trans*	Thomas et al., 1986

(*a*) The 669 cm^{-1} band of fd is proposed as a composite of dT (C2′-endo/anti) and dG (C3′-endo/anti) markers. In extracted fd DNA, well-resolved markers are observed at 668 (dT) and 682 (dG) cm^{-1}, indicating exclusively C2′-endo/anti conformers in the protein-free molecule (K. Aubrey, and G. J. Thomas, Jr., unpublished results and manuscript in preparation). (*b*) The 746 cm^{-1} band is proposed as a composite of contributions from dT (C2′-endo/anti) and from the DNA backbone. (*c*) Very low intensity, corresponding to 20 ± 10% of DNA OPO groups. See text.

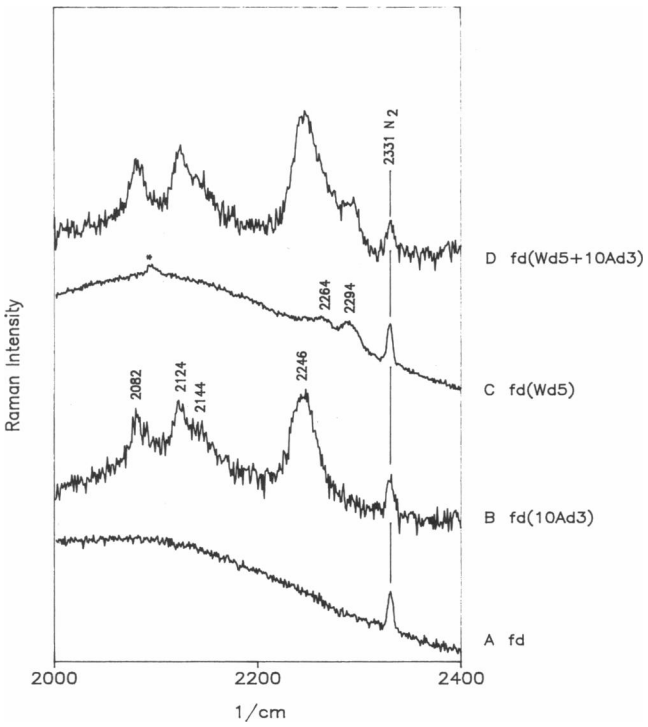

FIGURE 6 Raman spectra in the region 2,000–2,400 cm^{-1} of: (*A*) normal fd, (*B*) fd($10A_{d3}$), (*C*) fd(W_{d5}), and (*D*) fd(W_{d5} + $10A_{d3}$); obtained as indicated in Fig. 4. Spectral frequencies and intensities are scaled to the band at 2,331 cm^{-1} in each spectrum which is due to ambient N_2. The asterisk (*) indicates a laser artifact. All other bands are due to C-D stretching modes of deuterated side chains, as assigned in Table 1.

moderately hydrogen-bonded indoles in proteins, the band center is shifted to 877 cm^{-1}. Tryptophans which are exposed to water at the protein-solvent interface also exhibit σ_{17} near 877 cm^{-1}. For the very strong hydrogen bonds donated by indole 1N-H groups to carbonyl oxygens in crystalline structures, σ_{17} can be as low as 871 cm^{-1}. Therefore, the 876 cm^{-1} band of native fd shows that the hydrogen bond of the 1N-H group of W26 is of moderate strength. Although the specific hydrogen-bond acceptor for W26 is not identified in this study, the data are consistent with an oxy acceptor either of water or of a side-chain hydroxyl in the same or in a neighboring subunit. In a recently proposed model for the fd virion, Marvin has noted that the 1N-H group of W26 in a given protomer can donate a hydrogen bond to the phenoxyl group of Y21 in the neighboring, five-fold related, subunit (Marvin, 1990). The Raman frequency observed for σ_{17} in fd is consistent with this model.

The very intense tryptophan band near 1,360 cm^{-1} has been identified as one member of a Fermi doublet, with the companion member occurring near 1,340 cm^{-1} (Harada et al., 1986). The fundamental vibration involves mainly indole ring C2-C3 and C8-N stretching (Takeuchi and Harada, 1986). The relative intensity of the 1,360 cm^{-1} component ($I_{1,360}$), is a sensitive measure of the hydrophobicity or hydrophilicity of the indole ring environment (Miura et al., 1988). Hydrophobic interactions involving the indole ring and neighboring aliphatic or aromatic groups in a protein cause $I_{1,360}$ to achieve its maximum value. In a hydrophilic environment, including that of solvent-exposed tryptophan residues, $I_{1,360}$ is diminished and the band is significantly broadened. Remarkably, the W26 residue of the fd coat subunit is capable of exhibiting either a hydrophobic or hydrophilic indole ring environment depending upon the solution ionic strength (Thomas et al., 1983). At high ionic strengths, the 1,360 cm^{-1} band is sharp and intense; at the low-to-moderate salt conditions employed here, the band is weak, broad and barely discernible from the band contour which overlaps its low frequency side (Figs. 3 and 5). We conclude that, at low-salt (physiological) conditions, the molecular environment of the W26 indole ring is hydrophilic; however, at elevated salt conditions the Raman evidence clearly indicates a more hydrophobic environment for the W26 indole ring. Thus, the salt-induced structure transition noted previously for fd (Thomas et al., 1983) results in a significant qualitative change in microenvironment of W26. Others have noted that fluorescence and CD properties of W26 are suggestive of a hydrophobic environment (Day et al., 1979), which would appear to correlate well with the high-salt structure identified by Raman spectroscopy. We point out that considerably different experimental conditions are employed in absorption and Raman spectroscopies, viz. several orders of magnitude higher sample concentration for the latter, and these are close

to the effective viral concentrations in fibers examined by x-ray diffraction methods. We expect the hydrophilic environment of W26 identified here, rather than the hydrophobic state implied from CD and UV studies, to more closely resemble the conditions employed in x-ray fiber diffraction analyses. We note that the conformation-sensitive bands of fd near 876, 1,336 and 1,560 cm^{-1} also reflect the salt-induced change of indole ring environment (Thomas et al., 1983).

The normal mode σ_3, which involves mainly C9 = C4 ring double-bond stretching, is expected in the interval 1,540–1,560 cm^{-1}. The Raman frequency has been shown by combined x-ray/Raman analyses of model indole structures to be strongly dependent upon the torsion angle $X^{2,1}$ (Fig. 1), which defines the indole ring orientation about the C3-Cβ exocyclic bond (Miura et al., 1989). For gauche rotamers of the C2-C3-Cβ-Cα network ($X^{2,1} \sim \pm 60°C$), the center of the Raman band is expected near 1,540 cm^{-1}. On the other hand, for $X^{2,1} \sim \pm 120°C$, the Raman band center is expected near 1,558 cm^{-1}. This represents the upper limit of σ_3 observed among a large number of model compounds (Miura et al., 1989). For fd, we find the σ_3 mode of W26 located at 1,560 ± 1 cm^{-1}, which is essentially the upper limit. Accordingly, we conclude that the magnitude of the torsion angle $|X^{2,1}|$ is 120°C. This places the indole ring in a highly extended configuration with respect to the peptide main chain and constrains its plane to be nearly perpendicular to the local α-helical axis. $X^{2,1}$ values of ±120°C would appear to be consistent with 1N-H· · ·O hydrogen bonding between W26 and Y21 (Marvin, 1990). In accordance with Miura et al. (1989), we note that values of σ_3 near 1,552 cm^{-1} (corresponding to $X^{2,1} \sim \pm 90°C$) are most commonly observed in proteins. It is possible that the rather unusual indole ring orientation in protomers of fd is required for interaction with the ssDNA genome. This could also explain the rigorous requirement for W26 in phage assembly.

Conformations of packaged fd DNA

The present study reveals a broad Raman band centered near 746 cm^{-1}, which underlies the stronger tryptophan band of similar frequency. Present and previous results (Thomas et al., 1988) together show that it is unlikely the underlying 746 cm^{-1} band is due to tryptophan, tyrosine, phenylalanine, or any methyl side chain of gpVIII protomers. DNA assignment is strongly favored by the well catalogued Raman bands of thymidine (dT) and of the deoxyribose-phosphate backbone in the 740–770 cm^{-1} interval (Thomas and Benevides, 1985; Thomas et al., 1986; Katahira et al., 1986; Patapoff et al., 1988; Dijkstra et al., 1991). We assign the broad 746 cm^{-1} band primarily to DNA, and propose that it is the resultant of a thymidine contribution near 746 cm^{-1} and a phosphodiester contribution near 758 cm^{-1}. (A band at ~758 cm^{-1} is evident in spectra of many DNA sequences and conformations, although its precise structural significance remains unclear.) The thymidine 746 cm^{-1} assignment implies that a significant proportion of dT adopts the C2′-endo/anti conformation in packaged fd DNA. Consistent with this interpretation is the broad band at 669 cm^{-1}, assigned in part to the C2′-endo/anti dT marker (Dijkstra et al., 1991). We find no evidence of a 777 cm^{-1} thymidine marker, as would be expected if dT residues adopted the C3′-endo/anti conformation (Thomas and Benevides, 1985; Dijkstra et al., 1991).

The present study also confirms assignment of the deoxyguanosine (dG) conformation marker of packaged fd DNA to the band at 669 cm^{-1} (Thomas et al., 1988). The location of this important dG marker band at 669 cm^{-1}, and especially the absence of a dG marker band near 682 cm^{-1}, shows that C3′-endo/anti, and not C2′-endo/anti, is the dominant conformation for dG nucleosides of packaged fd DNA. (As expected, the Raman spectrum of fd DNA extracted from the phage shows a prominent C2′-endo dG marker at 682 cm^{-1}, comparable in intensity to the thymidine 668 cm^{-1} marker. A detailed comparison of Raman spectra of packaged and unpackaged fd DNA will be reported elsewhere [K. Aubrey and G. J. Thomas, Jr., manuscript in preparation]) The dA and dC markers, though relatively intense and well resolved in the present spectra, do not provide unambiguous information regarding nucleoside conformations. Both C3′-endo and C2′-endo conformers of dA and dC are consistent with the observed markers, as indicated in Table 2. We note also that the relative intensities of all nucleoside conformation markers listed in Table 2 are consistent with the fd-DNA base composition (24% dA, 34% dT, 20% dG, 22% dC).

Finally, the present data confirm the absence of a well ordered DNA backbone in the packaged genome (Thomas et al., 1988). The fd spectrum lacks a marker of the high intensity anticipated for extensively ordered phosphodiester groups (OPO torsions α and ζ), as occur in B-form (g^-/g^-, 790 and 835 cm^{-1} markers) or A-form DNA (g^-/t, 807 cm^{-1} marker) (Thomas et al., 1986). In addition to the putative 758 cm^{-1} band discussed above, the Raman profile of fd in the 600–900 cm^{-1} interval contains only a very weak band near 806 cm^{-1} which can be reasonably assigned to the DNA mainchain (Thomas et al., 1988). The 806 cm^{-1} band is far too weak to signify backbone geometry of the A type throughout the fd genome, but can be interpreted as evidence of a small percentage (~20 ± 10%) of DNA OPO groups with torsions α and ζ in the gauche$^-$ and trans orientations, respectively. This is clearly consistent with the proposed

C3′-endo/anti dG conformers. The absence of an intense backbone marker in the region 800–840 cm^{-1} is characteristic of a broad distribution of α,ζ torsions. A similar Raman profile is observed for the packaged ssDNA genome of bacteriophage ϕX174 (Benevides et al., 1991a).

Implications for other residue assignments

In addition to the Raman bands of tryptophan and alanine isotopomers which are directly revealed by incorporation of labeled side chains into gpVIII, our spectral data suggest the possibility of indirect structural changes resulting from tryptophan deuteration. Fig. 5 shows that the phenylalanine band near 1,002 cm^{-1} is apparently perturbed in intensity by incorporation of W_{d5}. Although it will be necessary to design more precise experimental tests of these effects, the present results suggest at least the possibility that tryptophan ring deuteration may very weakly perturb intersubunit interactions involving the phenyl ring(s). In this regard we note that the fd assembly model proposed by Marvin (Marvin, 1990) locates the three phenyl rings (per subunit) in close proximity as follows: Residue F11 of a given subunit is tightly sandwiched between residues F42 and F45 of the 17TH neighboring subunit.

Future studies will focus on incorporation of additional deuterated side chains in gpVIII, including complete CD_3 incorporation (A + V + I + T + L + M), and deuterio-methylene incorporations, particularly CD_2 of K, R, S, D, E, Q, F, Y, W and P side chains.

The authors thank Dr. Loren A. Day, New York Public Health Research Institute, and Dr. Stanley J. Opella, University of Pennsylvania, for advising Kelly Aubrey in techniques for growth of normal and labeled fd. We also thank Ms. Stacy Towse and Drs. Charles J. Wurrey and James M. Benevides, University of Missouri at Kansas City, for helpful comments on the manuscript. This work constituted part of the thesis research of Kelly Aubrey for the M.S. degree in Microbiology. This research was supported by National Institutes of Health grant AI11855.

Received for publication 6 June 1991 and in final form 12 August 1991.

REFERENCES

Aubrey, K. 1990. In vivo incorporation of specifically deuterated amino acids into filamentous bacteriophage fd for Raman spectroscopic analysis. M.S. thesis. School of Basic Life Sciences, University of Missouri, Kansas City, Missouri.

Bellamy, L. J. 1980. The Infrared Spectra of Complex Molecules. *In* Advances in Infrared Group Frequencies, Second Edition. Chapman and Hall Publishers, New York.

Benevides, J. M., P. L. Stow, L. L. Ilag, N. L. Incardona, and G. J. Thomas, Jr. 1991*a*. Differences in secondary structure between packaged and unpackaged single-stranded DNA of bacteriophage ϕX174 determined by Raman spectroscopy: A model for ϕX174 DNA packaging. *Biochemistry.* 30:4855–4863.

Benevides, J. M., M. A. Weiss, and G. J. Thomas, Jr. 1991*b*. Design of the helix-turn-helix motif: Nonlocal effects of quaternary structure in DNA recognition investigated by laser Raman spectroscopy. *Biochemistry.* 30:4381–4388.

Bunow, M. R., and I. W. Levin. 1977. Raman spectra and vibrational assignments for deuterated membrane lipids. *Biochim. Biophys. Acta.* 489:191–206.

Cross, T. A., P. Tsang, and S. J. Opella. 1983. Comparison of protein and deoxyribonucleic acid backbone structures in fd and Pf1 bacteriophages. *Biochemistry.* 22:721–726.

Day, L. A., R. L. Wiseman, and C. J. Marzec. 1979. Structure models for DNA in filamentous viruses with phosphates near the center. *Nucl. Acids Res.* 7:1393–1403.

Day, L. A., and R. L. Wiseman. 1978. A comparison of DNA packaging in the virions of fd, Xf and Pf1. *In* The Single Stranded DNA Phages. D. T. Denhardt, D. Dressler, and D. S. Ray, editors. Cold Spring Harbor Laboratory Press, New York. 605–675.

Day, L. A., C. J. Marzec, S. A. Reisberg, and A. Casadevall. 1988*a*. DNA packing in filamentous bacteriophages. *Annu. Rev. Biophys. Biophys. Chem.* 17:509–539.

Day, L. A., A. Casadevall, B. Prescott, and G. J. Thomas, Jr. 1988*b*. Raman spectroscopy of mercury(II) binding to two filamentous viruses: Ff (fd, M13, F1) and Pf1. *Biochemistry.* 27:706–711.

Denhardt, D. T., D. Dressler, and D. S. Ray, editors. 1978. *In* The Single Stranded DNA Phages. Cold Spring Harbor Laboratory Press, New York.

Dijkstra, S., J. M. Benevides, and G. J. Thomas, Jr. 1991. Solution conformations of nucleoside analogues exhibiting antiviral activity against human immunodeficiency virus. *J. Mol. Struct.* 242:283–301.

Harada, I., T. Miura, and H. Takeuchi. 1986. Origin of the doublet at 1,360 and 1,340 cm^{-1} in the Raman spectra of tryptophan and related compounds. *Spectrochim. Acta.* 42A:307–312.

Kitagawa, T., T. Azuma, and K. Hamaguchi. 1979. The Raman spectra of Bence-Jones proteins. Disulfide stretching frequencies and dependence of Raman intensity of tryptophan residues on their environments. *Biopolymers.* 18:451–465.

Katahira, M., Y. Nishimura, M. Tsuboi, T. Sato, Y. Mitsui, and Y. Iitaka. 1986. Local and overall conformations of DNA double helices with A·T base pairs. *Biochim. Biophys. Acta.* 867:256–267.

Kuhn, A., J. Rohrer, and A. Gallusser. 1990. Bacteriophages M13 and Pf3 tell us how proteins insert into the membrane. *J. Struct. Biol.* 104:38–43.

Li, Y., G. J. Thomas, Jr., M. Fuller, and J. King. 1981. Investigations of bacteriophage P22 by laser Raman spectroscopy. *Prog. Clin. Biol. Res.* 64:271–283.

Makowski, L. 1984. Structural diversity in filamentous bacteriophages. *In* Biological Macromolecules and Assemblies: Virus Structures. F. A. Jurnak, and A. McPherson, editor. John Wiley and Sons Inc. New York. pp. 203–253

Makowski, L., and D. L. D. Caspar. 1981. The symmetries of filamentous phage particles. *J. Mol. Biol.* 145:611–617.

Marvin, D. A., R. L. Wiseman, and E. J. Wachtel. 1974*a*. Filamentous bacterial viruses. XI. Molecular architecture of the class II (Pf1, Xf) virion. *J. Mol. Biol.* 82:121–138.

Marvin, D. A., W. J. Pigram, R. L. Wiseman, E. J. Wachtel, and F. J.

Marvin. 1974*b*. Filamentous bacterial viruses. XII. Molecular architecture of the class I (fd, IF1, IKe) virion. *J. Mol. Biol.* 88:581–600.

Marvin, D. A. 1989. Dynamics of telescoping *Inovirus:* A mechanism for assembly at membrane adhesions. *Int. J. Biol. Macromol.* 11:159–164.

Marvin, D. A. 1990. Model-building studies of *Inovirus:* genetic variations on a geometric theme. *Int. J. Biol. Macromol.* 12:125–138.

Miura, T., H. Takeuchi, and I. Harada. 1988. Characterization of individual tryptophan side chains in proteins using Raman spectroscopy and hydrogen-deuterium exchange kinetics.

Miura, T., H. Takeuchi, and I. Harada. 1989. Tryptophan Raman bands sensitive to hydrogen bonding and side-chain conformation. *J. Raman Spectrosc.* 20:667–671.

Model, P., and M. Russel. 1988. Filamentous bacteriophage. *In* The Bacteriophages. R. Calendar, editor. Plenum Publishing Corp., New York. 375–456.

O'Leary, T. J., and I. W. Levin. 1986. Raman spectroscopy of selectively deuterated dimyristoylphosphatidylcholine: Studies on dimyristoylphosphatidylcholine–cholesterol bilayers. *Biochim. Biophys. Acta.* 854:321–324.

Opella, S. J., P. L. Stewart, and K. G. Valentine. 1987. Protein structure by solid-state NMR spectroscopy. *Quart. Rev. Biophys.* 19:7–49.

Patapoff, T. W., G. A. Thomas, Y. Wang, and W. L. Peticolas. 1988. Polarized Raman scattering from oriented single microcrystals of $d(A_5T_5)_2$ and d(pTpT). *Biopolymers.* 27:493–507.

Qian, W., J. Bandekar, and S. Krimm. 1991. Vibrational analysis of crystalline tri-L-alanine. *Biopolymers.* 31:193–210.

Siamwiza, M. N., R. C. Lord, M. C. Chen, T. Takamatsu, I. Harada, H. Matsuura, and T. Shimanouchi. 1975. Interpretation of the doublet at 850 and 830 cm^{-1} in the Raman spectra of tyrosyl residues in proteins and certain model compounds. *Biochemistry.* 14:4870–4876.

Takeuchi, H., and I. Harada. 1986. Normal coordinate analysis of the indole ring. *Spectrochim. Acta.* 42A:1069–1078.

Thomas, G. J., Jr. 1987. Viruses and nucleoproteins. *In* Biological Applications of Raman Spectroscopy: Raman Spectra and the Conformations of Biological Macromolecules. T. G. Spiro, editor. Wiley-Interscience, New York. 135–201.

Thomas, G. J., Jr., and P. Murphy. 1975. Structure of coat proteins in Pf1 and fd virions by laser Raman spectroscopy. *Science (Wash. DC).* 188:1205–1207.

Thomas, G. J., Jr., B. Prescott, and L. A. Day. 1983. Structure similarity, difference and variability in the filamentous viruses fd, If1, IKe, Pf1, Xf and Pf3: Investigation by laser Raman spectroscopy. *J. Mol. Biol.* 165:321–356.

Thomas, G. J., Jr., and J. M. Benevides. 1985. An A-helix structure for poly(dA-dT)·poly(dA-dT). *Biopolymers.* 24:1101–1105.

Thomas, G. J., Jr., B. Prescott, and J. M. Benevides. 1986. DNA and RNA structures in crystals, fibers and solutions by Raman spectroscopy with applications to nucleoproteins. *Biomolec. Stereodynamics.* 4:227–254.

Thomas, G. J., Jr., B. Prescott, S. J. Opella, and L. A. Day. 1988. Sugar pucker and phosphodiester conformations in viral genomes of filamentous bacteriophages: fd, If1, IKe, Pf1, Xf and Pf3. *Biochemistry.* 27:4350–4357.

Webster, R. E., and J. Lopez. 1985. Structure and assembly of the class I filamentous bacteriophage. *In* Virus Structure and Assembly. S. Casjens, editor. Jones and Bartlett, Boston. 235–267.